

VU Research Portal

Function and homeostasis of murine splenic dendritic cell subsets

Backer, R.A.

2009

document version

Publisher's PDF, also known as Version of record

[Link to publication in VU Research Portal](#)

citation for published version (APA)

Backer, R. A. (2009). *Function and homeostasis of murine splenic dendritic cell subsets*. [PhD-Thesis - Research and graduation internal, S.I.]. s.n.

General rights

Copyright and moral rights for the publications made accessible in the public portal are retained by the authors and/or other copyright owners and it is a condition of accessing publications that users recognise and abide by the legal requirements associated with these rights.

- Users may download and print one copy of any publication from the public portal for the purpose of private study or research.
- You may not further distribute the material or use it for any profit-making activity or commercial gain
- You may freely distribute the URL identifying the publication in the public portal

Take down policy

If you believe that this document breaches copyright please contact us providing details, and we will remove access to the work immediately and investigate your claim.

E-mail address:

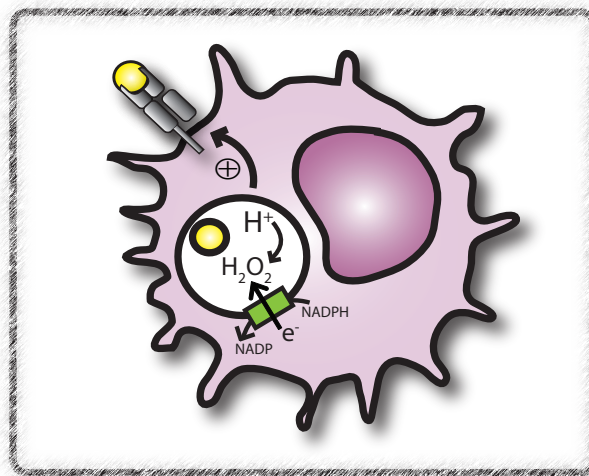
vuresearchportal.ub@vu.nl

CHAPTER 4

NADPH oxidase-derived reactive oxygen species enhance antigen cross-presentation of dendritic cells

Ronald Backer¹, Georg Kraal¹ & Joke M.M. den Haan¹

¹Dept. Molecular Cell Biology and Immunology, VU University Medical Center, Amsterdam



4.1 ABSTRACT

Alkalinisation of DC phagosomes determines the cross-presentation capacity of DCs by preventing total degradation of internalized proteins. We observed that CD8⁻ DCs express higher levels of the NOX2 subunits gp91^{phox}, p40^{phox} and p67^{phox} as compared to CD8⁺ DCs. This correlated with higher NOX2 activity after PMA and yeast stimulation in the CD8⁻ DC subset. The role of ROS on Ag-presentation was investigated by using the NADPH oxidase inhibitor apocynin. Inhibition of ROS production reduced MHC class I related cross-presentation about 3-fold, while the classical MHC class II presentation was less sensible to apocynin. Together, our data identified a role of NOX2 activity in Ag-presentation by DCs.

4.2 INTRODUCTION

Antigens (Ags) that are taken up by professional antigen-presenting cells (APCs) end up in endosomal or phagosomal compartments. Macrophages (M ϕ) and neutrophils use proteolysis for pathogen killing and clearance of internalized structures. During phagosome-maturation, these cells recruit V-ATPases to their phagosomes. This results in acidification of phagosomes. Due to this low pH, Ags are denatured and destructed by proteases, which are strongly activated under acidic conditions. However, for Ag-presentation, proteins have to be converted into peptides that bind to MHC molecules for display at the cell surface. This indicates that the initial degradation of Ags in phagosomes has to be tightly controlled, and important T cell epitopes must avoid complete destruction by proteases before association with MHC molecules.

Among APCs, dendritic cells (DCs) are potent Ag-presenting cells. DCs are the main cell type involved in cross-presentation. For optimal Ag-processing and Ag-presentation, DCs adapted their phagosomal pathway in such a way that their potency to degrade Ags is low. To control Ag degradation, DCs express lower levels of lysosomal enzymes as compared to M ϕ ¹. DCs also show inefficient acidification of phagosomes due to low V-ATPase activity² and due to RAB27a dependent recruitment of NADPH oxidases to phagosomes³. The recruited NADPH oxidase generates an alkalic pH that is actively maintained in DC phagosomal compartments. Reports show that neutralization of the endosomal/phagosomal pH resulted in attenuated proteolysis and prolonged persistence of Ags, improving Ag-presentation in DCs⁴. This Ag-preservation in DCs clearly illustrates the different roles of DCs and M ϕ in the immune system. Phagosome-maturation in M ϕ serves to remove pathogens and other potentially dangerous particles by proteolysis, while DCs are not directly involved in pathogen clearance. Phagosome-maturation in DCs serves to process Ags rather than complete degradation favouring Ag presentation.

NOX2 is a major source of reactive oxygen species (ROS) and is part of the phagocytic NADPH oxidase (NOX) family^{5;6}. NOX2 is a multi-component enzyme complex consisting of membrane-bound catalytic heterodimer flavocytochrome b_{558} (p22^{phox} and gp91^{phox}) and the cytosolic components p40^{phox}, p47^{phox} and p67^{phox} 7;8. In resting cells, the subunits are disassembled and inactive. Following activation, the cytosolic components translocate to the membrane and assemble into a functional complex⁹⁻¹¹. The small GTPases RAC-1 and RAC-2 are the major adaptors involved in the interaction of p67^{phox} with cytochrome b_{558} ¹²⁻¹⁴. RAC-1

is ubiquitously expressed and is mainly involved in non-phagocytic NADPH activation¹⁴, while RAC-2 regulates NADPH oxidase activity after phagocytosis by hematopoietic cells^{15;16}. Once assembled, the NADPH oxidase forms a respiratory chain that transports single electrons from the cytoplasmic donor NADPH across endocytic membrane to molecular oxygen¹⁷. The generated superoxide anions ($O_2^{\cdot-}$) subsequently dismutate into hydrogen peroxide (H_2O_2) and other ROS species. The consumption of protons (H^+) during this process is causing an increase of phagosomal pH, generating a milieu where proteolytic enzymes are not optimally active^{18;19}.

In the mouse spleen, different DC subpopulations can be identified. These $CD8^+$ and $CD8^-$ DCs differ in their Ag-presentation and T cell activation capacity. The $CD8^+$ DC subset is very well able to cross-present many kinds of Ag^{20;21}, while $CD8^-$ DCs are only known to cross-present immune-complexes and yeast-derived Ags^{22;23}.

In this study we aimed to elucidate the role of NOX2-dependent ROS production on presentation of soluble and yeast-derived Ag splenic DC subsets. Our results indicate that yeast efficiently induced ROS in $CD8^-$ DCs, which express higher levels of NOX2 subunits as compared to $CD8^+$ DCs. Furthermore, Ag-presentation by splenic DCs was studied in the absence or presence of apocynin, an agent inhibiting ROS production by the NADPH oxidase complex. Apocynin was able to reduce Ag-presentation by DCs, indicating an important role of ROS in determining Ag-presentation efficiencies by DCs.

4.3 MATERIALS AND METHODS

Mice

C57Bl/6-J (B6) mice, 8-16 weeks of age, were obtained from Charles River (L'Arbresle, France). OT-I and OT-II mice were bred at the animal facility of the VU University Medical Center (Amsterdam, The Netherlands). OT-I and OT-II mice have transgenic $V\alpha 2V\beta 5$ T cell receptors that recognize the OVA₂₅₇₋₂₆₄ peptide in the context of H2-K^b and the OVA₃₂₃₋₃₃₉ peptide in the context of I-A^b, respectively. All mice were kept under specific pathogen-free conditions and used in accordance of local animal experimentation guidelines.

Media, reagents and mAbs

Culture medium was Iscove's modified Dulbecco's medium (IMDM; Gibco, Paisley, UK) supplemented with 10% heat-inactivated FCS, 200 U/ml penicillin, 200 μ g/ml streptomycin (BioWhittaker), 4 mM L-glutamin (BioWhittaker) and 50 μ M β -mercaptoethanol (Fluka) (IMDM/DC). For DC isolation and MACS purification, 10 mM EDTA/ 20 mM Hepes was added (IMDM/HE). Monoclonal antibodies (mAb) were used for flowcytometry and in blocking experiments. Anti-CD8 α (clone 53-6.7) and anti-CD11c (clone N418) were obtained from eBioscience (San Diego, CA).

The OVA-expressing *Saccharomyces cerevisiae* (yeast-OVA) used in this study was generated as described before²³. OVA-immune complexes (OVA-IC) were generated by incubating 10 μ g/ml OVA (Calbiochem) or 3-fold dilutions together with polyclonal rabbit anti-OVA IgG (25 μ g/ml) for 30 min at 37°C. The mAbs NLDC145 (specific for DEC205), 33D1 (specific for DCIR2) and R7D4 (negative control recognizing an idiotypic determinant on a mouse B cell lymphoma) were covalently coupled to OVA as described before [Backer *et al.* manuscript in preparation]. In short, mAbs coupled to a No-Weight™ Sulfo-SMCC linker (Pierce) were incubated with OVA-DTT. The coupling reaction was stopped by adding 1 mM L-cysteine solution and non-coupled OVA was removed by protein-G purification.

Apocynin (4-hydroxy-3-methoxyacetophenone, acetovanillone; Sigma, St Louis, MO, USA), a selective inhibitor of NADPH oxidase, was dissolved in PBS and used *in vitro* in a concentration of 333 μ M.

DC isolation and cell sorting

Spleens of 5–15 B6 mice were cut into grain size pieces and incubated in 1 ml per spleen of 1 WU/ml Liberase I (Roche Diagnostics GmbH,

Mannheim, Germany) and 50 µg/ml DNase I (Roche) in medium without FCS and β-mercaptoethanol with continuous stirring at 37°C for 30 min or until digested. EDTA was added to a 10 mM final concentration, and the cell suspension was incubated for an additional 5 min at 4°C. Red blood cells were lysed with ACK lysis buffer. Cells were washed once with IMDM/HE and undigested material was removed by filtration. DCs were purified by positive selection with anti-CD11c MACS microbeads (Miltenyi Biotec, Bergisch Gladbach, Germany) following manufacturer's protocol.

MACS purified DCs were stained for CD11c and CD8 and then subsequent cell sorting was performed with Moflow (Dako Cytomation) in HBSS with 25 mM Hepes by gating on high expression of CD11c and the absence or presence of CD8. Auto-fluorescent cells were excluded. Purity and viability of the sorted samples was determined by re-analysis on the cell-sorter. Sorting for CD8⁻ and CD8⁺ DC populations resulted in 90-95% pure populations.

Isolation of T cells

CD8⁺ T cells and CD4⁺ T cells were isolated from spleen and lymph nodes (LNs) of OT-I and OT-II transgenic mice, respectively, and single cell suspensions were obtained. Specific T cells were purified by negative depletion using bead-based T cell isolation kits (DynaL Biotec ASA, Oslo, Norway) following manufacturer's protocols. Purity of T cell preparations was between 80 and 90%.

Quantitative real-time PCR analysis of NADPH oxidase subunit expression

Total RNA was prepared with TRIzol reagent (Invitrogen) from sorted CD8⁺ and CD8⁻ DCs. The cDNA was synthesized from total RNA with random hexamers and M-MuLV reverse transcriptase (Fermentas). Quantitative PCR was determined with PowerSYBRGreen (AB Applied Biosystems, Warrington, UK) incorporation for p22^{phox}, p40^{phox}, p47^{phox}, p67^{phox} and gp91^{phox} on an ABI Prism 7900HT Sequence Detection System (Applied Biosystems). Results were normalized to those obtained with HPRT and results are presented as relative quantities of mRNA.

Detection of H₂O₂ Production

5×10⁴ FACS sorted DCs were stimulated by adding yeast-OVA (10⁵/well) or with PMA (50 ng/ml) in the absence or presence of apocynin. The rate of H₂O₂ production was determined using the oxidation of

the fluorogenic indicator Amplex Red (0.1 unit/ml) in the presence of horseradish peroxidase (50 M). Fluorescence was recorded over time in a FluorStar spectrofluorimeter (BMG Labtec, Offenburg, Germany) with 535 nm excitation and 595 nm emission wavelengths. Standard curves, obtained by adding 0-10 μM H_2O_2 to assay medium in the presence of the reactants (Amplex-red and horseradish peroxidase), were linear up to 2 M.

Cross-presentation assay

To detect Ag-presentation, DCs were used as stimulators for naive T cells in a [^3H]-thymidine incorporation assay. For this, 10^5 CD11c⁺ DCs were co-incubated with varying numbers of yeast-OVA, soluble OVA or OVA-IC in the presence of 10^5 purified OT-1 CD8⁺ T cells, or 10^5 purified OT-II CD4⁺ T cells in triplicate in flat-bottomed 96-wells plates (Nunc). To target specifically to CD8⁺ or CD8⁻ DCs, OVA chemically coupled to αDEC205 or αDCIR2 was added, respectively. To inhibit the NADPH oxidase complex, apocynin (333 μM) was added to the wells. As a positive control, stimulator cells were coated with 1 $\mu\text{g}/\text{ml}$ MHC class I OVA₂₅₇₋₂₆₄ peptide or 10 $\mu\text{g}/\text{ml}$ MHC class II OVA₃₂₃₋₃₃₉ peptide for 1 h and washed three times. After 48 h incubation in a CO_2 incubator, plates were pulsed with 1 $\mu\text{Ci}/\text{well}$ of [^3H]-thymidine. After additional 16 h of incubation, [^3H]-thymidine incorporation was measured on a Wallac-LKB Betaplate 1205 liquid scintillation counter. Data were summarized by the mean and standard error of the mean (SEM).

4.4 RESULTS

NADPH oxidase subunits are differentially expressed by splenic DC subsets

Splenic CD8⁺ and CD8⁻ DCs differ in their capacity to cross-present given types of Ag²⁴⁻²⁶. Since the NADPH oxidase NOX2 is important for the regulation of cross-presentation by controlling phagosomal pH⁴, we set out to study the expression of NOX2 by CD8⁺ and CD8⁻ DCs. NOX2 consists of several subunits (Figure 1A). Quantitative PCR revealed a higher expression of the gp91^{phox} subunit in CD8⁻ DCs as compared to CD8⁺ DCs (Figure 1B). Also other subunits of the NOX2 complex were expressed by both DC subsets, although with a profound higher expression of p40^{phox} and p67^{phox} within CD8⁻ DCs (Figure 1C,D). The expression of p22^{phox} and p47^{phox} were comparable between the DC subsets (Figure 1E, F).

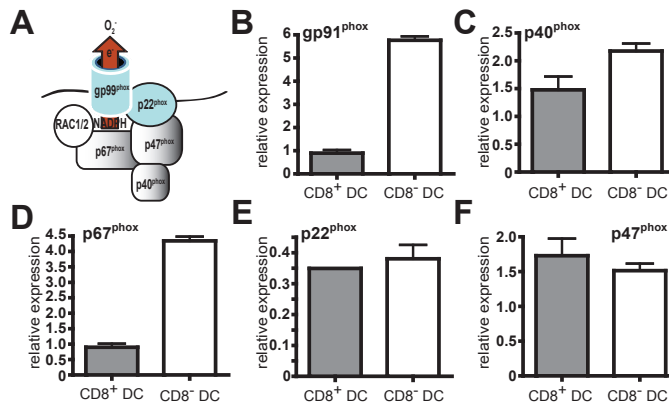


[Figure 1] CD8⁻ DCs specifically express high levels of NADPH oxidase components. (A) Schematic representation of the NADPH oxidase complex NOX2. NOX2 consists of 2 membrane-associated subunits (gp91^{phox} and p22^{phox}) which after activation recruit the cytosolic components p40^{phox}, p47^{phox} and p67^{phox} together with RAC1/2. The assembled complex allows transfer of electrons from NADPH to molecular oxygen. (B-F) CD11c^{high} CD8⁺ (gray bars) and CD8⁻ (white bars) DCs were FACS sorted and mRNA was subjected to quantitative real-time-PCR analysis to determine mRNA levels of gp91^{phox}, p22^{phox}, p40^{phox}, p47^{phox} and p67^{phox}, as indicated. Expression values are normalized to HPRT.

Since gp91^{phox}-deficient BM-DCs showed an increased phagosomal acidification as compared to wt BM-DCs⁴, the differential expression of NOX2 components between DC subsets suggested differential capacities to produce ROS. To study the functional consequences of the differential expression of NOX2 components, FACS sorted CD8⁺ and CD8⁻ DCs were stimulated with PMA. As shown in Figure 2A, CD8⁻ DCs were more active in the production of total cellular ROS over time after PMA stimulation

than CD8⁺ DCs, although the measured levels of ROS were a fraction of these produced by splenic M ϕ (data not shown). The higher capacity of ROS production by CD8⁻ DCs is clearly shown when the production rate per minute was calculated (Figure 2B). These results show that more NADPH oxidase activity is present in CD8⁻ DCs and that CD8⁻ DCs are more efficient in generating total ROS.

DCs, and preferentially CD8⁻ DCs, are able to cross-present yeast derived Ags²³. To determine whether yeast stimulation activates NOX2 in splenic DCs, we measured the oxidative burst in FACS sorted DC subsets induced by yeast (Figure 2C). Yeast indeed efficiently induced ROS production by DCs over time. Notably, the oxidative burst of CD8⁻ DCs was significantly higher than that of CD8⁺ DCs.

Apocynin is an efficient inhibitor of the NADPH oxidase activity. To test the inhibitory effect of apocynin on ROS production, ROS production by Flt3L generated BM-DCs in the absence or presence of apocynin (Figure 2D). Treatment of BM-DCs with apocynin induced a marked decrease of ROS production over time by both DC subsets after PMA stimulation in a dose dependent manner. At a concentration of 333 μ M, apocynin was able to completely inhibit ROS formation by BM-DCs. Based

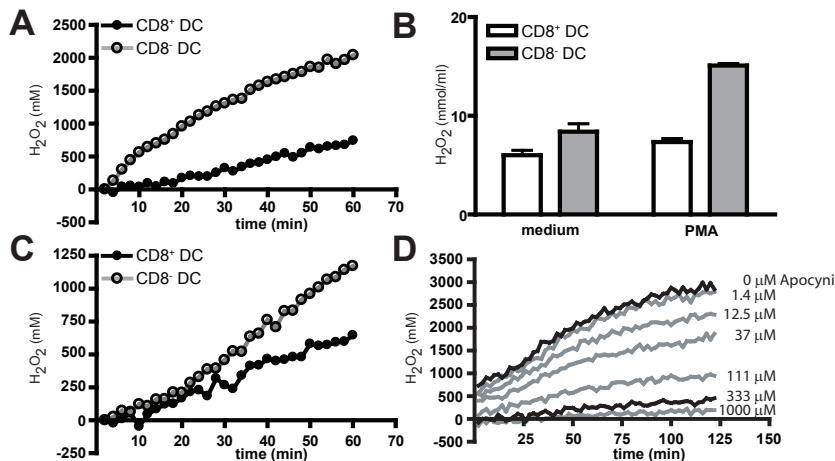


[Figure 2] PMA and yeast preferentially activate ROS production in CD8⁻ DCs.

(A) FACS sorted CD11c^{high} CD8⁺ (black line) and CD8⁻ (gray line) DCs were stimulated with 100 nmol/ml PMA. Subsequent ROS production was measured over time by an Amplex-red based luminescence assay. **(B)** Bars represent the mean rate of ROS production with or without PMA stimulation. **(C)** CD11c^{high} CD8⁺ (black lines) and CD8⁻ (gray lines) DCs were co-incubated with OVA expressing yeast and subsequent NOX2 activation was determined by measuring ROS production over time by Amplex-red. **(D)** Apocynin, an efficient inhibitor of NADPH oxidase, was added to FLT3 generated BM-DCs and the ability to inhibit ROS production after PMA stimulation was assayed by Amplex-red. The black lines indicate the concentrations of apocynin used in further experiments. Error bars indicate SEM of triplicate wells. Data are representative of two independent experiments.

on these results, we decided to use apocynin at concentrations of 333 μ M to investigate the effect of NOX2 inhibition on Ag-presentation in the following experiments.

Decreased Ag presentation of OVA-IC and yeast-OVA after inhibition of ROS production

Given that yeast is an effective inducer of ROS, we hypothesized that cross-presentation of yeast-derived ovalbumin (OVA) by DCs is dependent on ROS production. To study the involvement of ROS in presentation of yeast derived Ags, splenic DCs were treated with or without apocynin and incubated with OVA-expressing *S. Cerevisiae* (yeast-OVA). Yeast-OVA was presented very efficiently by DCs, resulting in strong proliferation of both OT-I (Figure 3A) and OT-II T cells (Figure 3B) *in vitro*. OT-I T cell proliferation was about 3-fold inhibited in the presence of apocynin (Figure 3A), while MHC class II presentation of yeast-OVA was less sensitive to apocynin (Figure 3B). Apocynin was not able to block cross-presentation by DCs completely, while at the concentrations used, PMA-induced ROS was completely inhibited (Figure 2D).

Also immune-complexes are an efficient source of Ag for cross-presentation^{22;23}. Ag-presentation of immune-complexes in the absence or presence of apocynin was analyzed by incubating DCs with OVA-ICs containing titrated amounts of OVA protein and a fixed concentration of OVA-specific rabbit IgG. OVA-IC was efficiently presented in the context of both MHC class I and MHC class II (Figure 3C,D). At the same concentrations, soluble OVA did not induce any detectable T cell proliferation (Figure 3C,D). Interestingly, cross-presentation of OVA-ICs was partially inhibited in the presence of apocynin (Figure 3C), while MHC class II presentation and subsequent CD4⁺ T cell activation was not affected (Figure 3D).

Importantly, DCs pulsed with the relevant synthetic MHC class I and class II OVA peptides OVA-peptides showed similar T cell priming efficiencies in the absence or presence of apocynin. This demonstrated that the presence of apocynin specifically affected Ag-processing by DCs and did not have an effect on T cell priming and T cell activation (Figure 3E,F).

Cross-presentation of DEC205 targeted OVA is ROS independent

Previous *in vivo* experiments were performed with a mixture of total CD11c⁺ DCs isolated from the mouse spleen. To investigate the role of NOX2 derived ROS on Ag-presentation by CD8⁺ and CD8⁻ DCs individually,

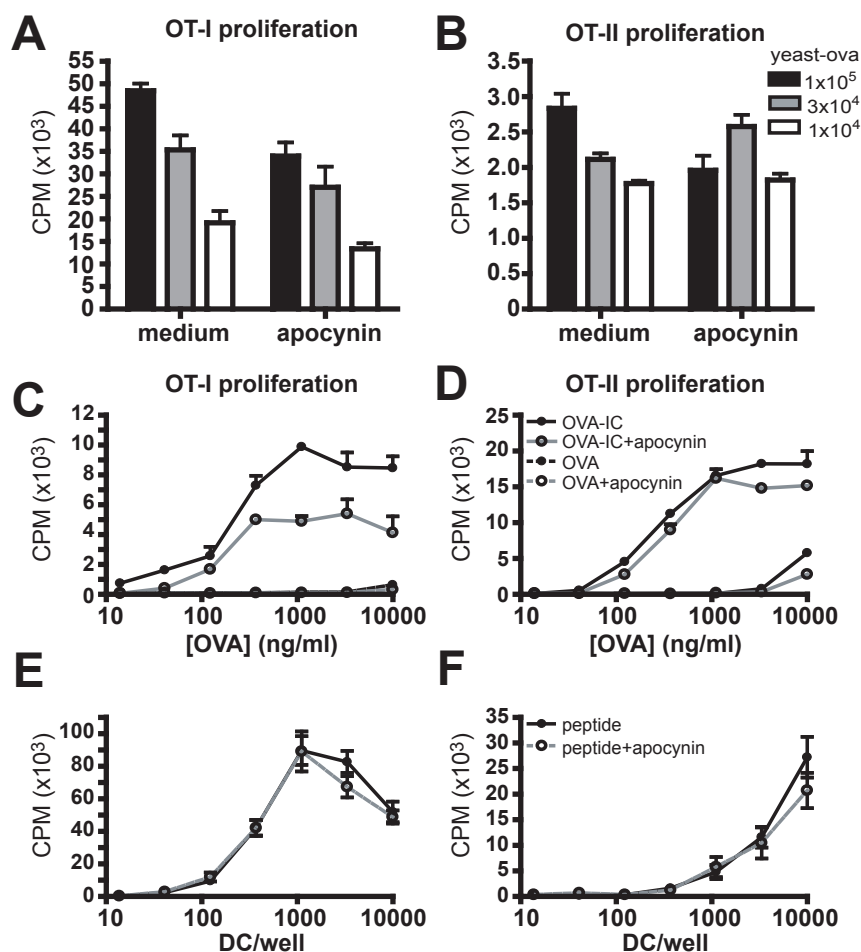


[Figure 3] MHC class I Ag-presentation of yeast and immune complexes is ROS dependent.

Single cell suspensions were obtained from mouse spleens and CD11c⁺ DCs were purified by MACS. DCs were incubated with yeast-OVA in absence or presence of 333 μ M apocynin. Purified OT-I CD8⁺ T cells or OT-II CD4⁺ T cells were added, and after 2 days, cultures were pulsed with 1 μ Ci [³H]-thymidine. OT-I (**A**) and OT-II (**B**) T cell proliferation was measured after an additional co-culture of 16 hr. Bars indicate a 1:3 titration of yeast-OVA. (**C**) DCs were incubated with OVA-ICs (solid lines) or soluble OVA (dotted lines) and subsequent OT-I T cell proliferation in the absence or presence of apocynin was determined by [³H]-thymidine. In the assay, the amount of OVA was titrated. (**D**) Same experimental setup, but now OT-II T cell proliferation was determined. As control, DCs were coated with MHC class I OVA₂₅₇₋₂₆₄-peptide (**E**) or MHC class II OVA₃₂₃₋₃₃₉ peptide (**F**) and presentation in the absence or presence of 333 μ M apocynin was assessed through T cell proliferation. Error bars indicate SEM of triplicate wells. Data are representative of two independent experiments. ***P < 0.001 versus medium control. P values were calculated by one-way ANOVA with Bonferroni correction (GraphPad Prism 4 software).

we decided to *in vitro* target OVA specifically to either DC subset. In order to target CD8⁺ and CD8⁻ DCs, OVA was chemically linked to antibodies (mAb) recognizing DEC205 or DCIR2, respectively.

Incubation with the control mAb-OVA complex did not result strong proliferation of OT-I (Figure 4A) or OT-II T (Figure 4B) T cells, indicating that mAb-OVA induced T cell proliferation was not due to non-targeted uptake by Fc-receptors. Targeting CD8⁺ DCs with α DEC205-OVA resulted in strong OT-I and OT-II T cell proliferation. We observed that neither OT-I nor OT-II T cell proliferation could be inhibited in the presence of apocynin (Figure 4A,B). This indicates that processing and presentation of DEC205 targeted Ags was independent of inhibition of NOX2 activity by apocynin.

CD8⁻ DCs were not very efficient in the activation of OT-I T cells as described before after incubation with α DCIR2-OVA (Figure 4A), while efficient OT-II proliferation was observed (Figure 4B)²⁶. Due to the absence or low OT-I T cell proliferation, no effect of apocynin could be

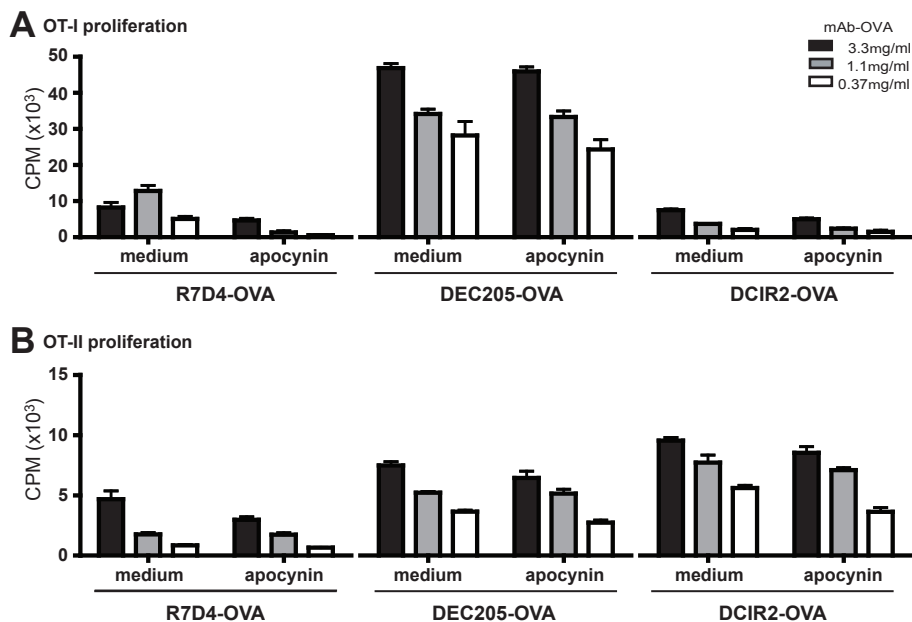


[Figure 4] Cross-presentation of DC targeted Ag is ROS independent.

CD11c⁺ DCs were co-cultured with the indicated mAb-OVA, together with purified OT-I (**A**) or OT-II (**B**) T cells in the absence or presence of 333 μ M apocynin. After 2 days, cultures were pulsed with 1 μ Ci [³H]-thymidine/well. T cell proliferation was measured after an additional co-culture of 16 h. Different bars indicate titration of mAb-OVA complexes in the assay. Error bars indicate SEM of triplicate wells.

detected on cross-presentation of α DCIR2-OVA by this DC subset (Figure 4A), but MHC class II restricted Ag-presentation was observed to be ROS independent (Figure 4B).

4.5 DISCUSSION

CD8⁺ and CD8⁻ DC subsets in the mouse spleen show distinct capacities for the activation of CD8⁺ and CD4⁺ T cells^{25;26}. The observed specialization for cross-presentation by CD8⁺ DCs has been explained by the higher expression of genes involved in the MHC class I restricted Ag-presentation pathway²⁶, whereas a recent study reports selective RAC2 dependent recruitment of NOX2 subunits to the phagosome in CD8⁺ DCs²⁷. NOX2 has been shown to be required for efficient Ag-presentation via the production of ROS. ROS prevent phagosomal acidification, thereby tightly controlling Ag-degradation^{3;4;27}. In CD8⁺ DCs, RAC2 mediates the assembly of NOX2 at the membrane of the phagosome, while in CD8⁻ DCs RAC1 regulates NOX2 assembly at the cell membrane²⁷. This indicates, that although CD8⁻ DCs express higher levels of NOX2 components, the produced ROS is mainly secreted, while ROS in CD8⁺ DCs is localized in the phagosomes.

Under specific conditions, CD8⁻ DCs are able to cross-present Ags to CD8⁺ T cells, indicating that the cross-presentation processing machinery is fully functional in CD8⁻ DCs. We assume that this machinery has to be activated in CD8⁻ DCs. Treatment of DCs with yeast strongly induced the release of ROS due to the activation of the NADPH oxidase. Interestingly, yeast is an Ag substrate efficiently cross-presented preferentially by CD8⁻ DCs²³. Another Ag cross-presented by CD8⁻ DCs are immune-complexes²². Both types of Ag are taken up via receptors on DCs, dectin-1 and FcγR, respectively, that contain an ITAM-motif and signal via the adaptor protein Syk²⁸⁻³¹. ITAM-mediated Syk signalling is a potential activator of ROS production in Mφ³². Syk activates the guanine exchange factor (GEF) Vav that in turn activates RAC. Interestingly, Vav deficient DCs show a strong defect in cross-presentation³³. We hypothesize that recruitment of NOX2 to the phagosomes is normally inefficient in CD8⁻ DCs, but that Syk-Vav-Rac signalling can induce the localization of ROS production in phagosomes. This would improve processing and cross-presentation of phagocytosed Ags by the CD8⁻ DC subset.

We show that cross-presentation of DEC205 targeted OVA by CD8⁺ DCs was not affected by apocynin, indicating that targeting DEC205 did not result in NOX2 activation. Furthermore, while ROS production by DCs was completely abrogated, inhibition of NOX2 by apocynin only partially reduced antigen-presentation of yeast-OVA and OVA-IC. Apocynin inhibits NOX2 assembly, but only after pre-activation by H₂O₂ and peroxidases³⁴. Supposed that apocynin was completely active in DCs, our data suggest that cross-presentation is only partially dependent on

ROS. This is in line with reports, where cross-presentation by gp91^{phox}^{-/-} BM-DCs was studied⁴. Cross-presentation in the absence of gp91^{phox} was strongly inhibited, but not completely blocked, indicating that other pathways are involved in the regulation of Ag-presentation by DCs. Cross-presentation by DCs from RAC2 or from Vav deficient mice, however, was completely abrogated indicating the presence of NOX2 independent pathway of regulation^{27;33}. Another mechanism involved in the regulation of phagosomal pH is the activity of V-ATPases, however the role and regulation of these electron-transporters in Ag-presentation by DCs is not known. In conclusion, more research on NOX2 activity and possible other regulatory mechanisms in DCs is required.

Interestingly, our data showed that if NADPH oxidase generated ROS was influencing Ag-presentation, it was mainly affecting the cross-presentation capacities of DCs, while the ROS dependence of MHC class II presentation was not as clear. This suggest that the efficiency of the generation of MHC class I restricted peptides is more dependent on the phagosomal/endosomal pH, than MHC class II restricted peptides. It has been proposed that processing of MHC class II restricted peptides is less sensitive for phagosomal pH, since MHC class II molecules bind relative large peptides³⁵. These peptides are trimmed into required length by Cathepsin-S once bound to a MHC class II molecule. Binding to MHC class II protects the relevant epitopes from degradation³⁶ and therefore they are not as sensitive as MHC class I peptides for phagosomal pH.

In summary, this study reports that NOX2 is involved in selectively regulating Ag-presentation by DCs. Inhibition of ROS production reduced the efficiency of cross-presentation by DCs. Further research will be necessary to elucidate the role of NOX2 and other mechanism in cross-presentation by CD8⁺ and CD8⁻ DC subsets.

4.6 ACKNOWLEDGEMENTS

This work was supported by grand NWO917.46.311 from the Dutch Scientific Research program. We thank the staff of our animal facility for the care of the animals used in this study. We thank T. O'Toole for expert technical assistance during FACS sorting.



REFERENCE LIST

1. Lennon-Dumenil AM, Bakker AH, Maehr R et al. Analysis of protease activity in live antigen-presenting cells shows regulation of the phagosomal proteolytic contents during dendritic cell activation. *J.Exp.Med.* 2002;196:529-540.
2. Trombetta ES, Ebersold M, Garrett W, Pypaert M, Mellman I. Activation of lysosomal function during dendritic cell maturation. *Science* 2003;299:1400-1403.
3. Jancic C, Savina A, Wasmeier C et al. Rab27a regulates phagosomal pH and NADPH oxidase recruitment to dendritic cell phagosomes. *Nat.Cell Biol.* 2007;9:367-378.
4. Savina A, Jancic C, Hugues S et al. NOX2 controls phagosomal pH to regulate antigen processing during crosspresentation by dendritic cells. *Cell* 2006;126:205-218.
5. Cross AR, Segal AW. The NADPH oxidase of professional phagocytes--prototype of the NOX electron transport chain systems. *Biochim.Biophys.Acta* 2004;1657:1-22.
6. Vignais PV. The superoxide-generating NADPH oxidase: structural aspects and activation mechanism. *Cell Mol.Life Sci.* 2002;59:1428-1459.
7. Leusen JH, Verhoeven AJ, Roos D. Interactions between the components of the human NADPH oxidase: intrigues in the phox family. *J.Lab Clin.Med.* 1996;128:461-476.
8. Wientjes FB, Segal AW. NADPH oxidase and the respiratory burst. *Semin.Cell Biol.* 1995;6:357-365.
9. Segal AW, Abo A. The biochemical basis of the NADPH oxidase of phagocytes. *Trends Biochem.Sci.* 1993;18:43-47.
10. DeLeo FR, Quinn MT. Assembly of the phagocyte NADPH oxidase: molecular interaction of oxidase proteins. *J.Leukoc.Biol.* 1996;60:677-691.
11. Babior BM. NADPH oxidase. *Curr. Opin.Immunol.* 2004;16:42-47.
12. Bokoch GM, Diebold BA. Current molecular models for NADPH oxidase regulation by Rac GTPase. *Blood* 2002;100:2692-2696.
13. Diebold BA, Bokoch GM. Molecular basis for Rac2 regulation of phagocyte NADPH oxidase. *Nat. Immunol.* 2001;2:211-215.
14. Hordijk PL. Regulation of NADPH oxidases: the role of Rac proteins. *Circ.Res.* 2006;98:453-462.
15. Glogauer M, Marchal CC, Zhu F et al. Rac1 deletion in mouse neutrophils has selective effects on neutrophil functions. *J.Immunol.* 2003;170:5652-5657.
16. Bokoch GM, Zhao T. Regulation of the phagocyte NADPH oxidase by Rac GTPase. *Antioxid.Redox. Signal.* 2006;8:1533-1548.
17. Schrenzel J, Serrander L, Banfi B et al. Electron currents generated by the human phagocyte NADPH oxidase. *Nature* 1998;392:734-737.
18. Nathan C. Neutrophils and immunity: challenges and opportunities. *Nat.Rev.Immunol.* 2006;6:173-182.
19. Bokoch GM. Regulation of innate immunity by Rho GTPases. *Trends Cell Biol.* 2005;15:163-171.
20. den Haan JM, Lehar SM, Bevan MJ. CD8(+) but not CD8(-) dendritic cells cross-prime cytotoxic T cells in vivo. *J.Exp.Med.* 2000;192:1685-1696.

Reactive oxygen species enhance cross-presentation by DCs

21. Pooley JL, Heath WR, Shortman K. Cutting edge: intravenous soluble antigen is presented to CD4 T cells by CD8⁻ dendritic cells, but cross-presented to CD8 T cells by CD8⁺ dendritic cells. *J.Immunol.* 2001;166:5327-5330.
22. den Haan JM, Bevan MJ. Constitutive versus activation-dependent cross-presentation of immune complexes by CD8(+) and CD8(-) dendritic cells in vivo. *J.Exp.Med.* 2002;196:817-827.
23. Backer R, van LF, Kraal G, den Haan JM. CD8⁻ dendritic cells preferentially cross-present *Saccharomyces cerevisiae* antigens. *Eur.J.Immunol.* 2008;38:370-380.
24. den Haan JM, Lehar SM, Bevan MJ. CD8(+) but not CD8(-) dendritic cells cross-prime cytotoxic T cells in vivo. *J.Exp.Med.* 2000;192:1685-1696.
25. Schnorrer P, Behrens GM, Wilson NS et al. The dominant role of CD8⁺ dendritic cells in cross-presentation is not dictated by antigen capture. *Proc.Natl.Acad. Sci.U.S.A* 2006;103:10729-10734.
26. Dudziak D, Kamphorst AO, Heidkamp GF et al. Differential antigen processing by dendritic cell subsets in vivo. *Science* 2007;315:107-111.
27. Savina A, Peres A, Cebrian I et al. The Small GTPase Rac2 Controls Phagosomal Alkalinization and Antigen Crosspresentation Selectively in CD8(+) Dendritic Cells. *Immunity.* 2009
28. Rogers NC, Slack EC, Edwards AD et al. Syk-dependent cytokine induction by Dectin-1 reveals a novel pattern recognition pathway for C type lectins. *Immunity.* 2005;22:507-517.
29. Brown GD. Dectin-1: a signaling non-TLR pattern-recognition receptor. *Nat.Rev.Immunol.* 2006;6:33-43.
30. Mina-Osorio P, Ortega E. Signal regulators in FcR-mediated activation of leukocytes? *Trends Immunol.* 2004;25:529-535.
31. Nimmerjahn F, Ravetch JV. Fc-receptors as regulators of immunity. *Adv.Immunol.* 2007;96:179-20
32. Underhill DM, Rosnagle E, Lowell CA, Simmons RM. Dectin-1 activates Syk tyrosine kinase in a dynamic subset of macrophages for reactive oxygen production. *Blood* 2005;106:2543-2550.
33. Graham DB, Stephenson LM, Lam SK et al. An ITAM-signaling pathway controls cross-presentation of particulate but not soluble antigens in dendritic cells. *J.Exp.Med.* 2007;204:2889-2897.
34. Simons JM, Hart BA, Ip Vai Ching TR, Van DH, Labadie RP. Metabolic activation of natural phenols into selective oxidative burst agonists by activated human neutrophils. *Free Radic.Biol.Med.* 1990;8:251-258.
35. Savina A, Amigorena S. Phagocytosis and antigen presentation in dendritic cells. *Immunol.Rev.* 2007;219:143-156.
36. Delamarre L, Pack M, Chang H, Mellman I, Trombetta ES. Differential lysosomal proteolysis in antigen-presenting cells determines antigen fate. *Science* 2005;307:1630-1634.

